

# Bright solitary waves of atomic Bose-Einstein condensates under rotation

N.A. Jamaludin<sup>1</sup>, N.G. Parker<sup>1,2</sup> and A.M. Martin<sup>1</sup>

<sup>1</sup> *School of Physics, University of Melbourne, Parkville, Victoria 3010, Australia.*

<sup>2</sup> *Department of Physics and Astronomy, McMaster University, Hamilton, Ontario, L8S 4M1, Canada.*

(Dated: October 24, 2018)

We analyse the rotation of bright solitary waves formed of atomic Bose-Einstein condensates with attractive atomic interactions. By employing a variational technique and assuming an irrotational quadrupolar flow field, we map out the variational solutions in the rotating frame. In particular, we show that rotation has a considerable stabilising effect on the system, significantly raising the critical threshold for collapse of the bright solitary waves.

PACS numbers: 03.75.Kk, 34.20.Cf, 47.20.-k

In recent years, bright solitary waves have been created using ultra-cold atomic Bose-Einstein condensates (BECs) [1, 2, 3]. Under attractive atomic interactions, these matter waves are self-trapped in the longitudinal direction [4, 5, 6, 7, 8] and are closely analogous to the classic one-dimensional soliton [9]. However, these states must be confined in the remaining directions by a waveguide and can retain three-dimensional effects. The most lucid example is the collapse instability: in 3D a homogeneous, untrapped BEC with attractive interactions is unstable to collapse [10] while the 1D limit is stable to collapse. The presence of external trapping stabilises the BEC up to a critical atom number (or interaction strength) before collapse is triggered, as demonstrated experimentally [11, 12]. The collapse instability has limited bright solitary wave (BSWs) experiments to only a few thousand atoms per BSW [1, 2, 3]. The BSW solutions, and their critical points, have been studied theoretically [5, 6, 7, 8], with variational approaches shown to give very good predictions. The collisions of BSWs, which show intriguing behaviour and may have applications in interferometry, are also prone to collapse instabilities [7, 8, 14, 15, 19]. As such, it is pertinent to consider approaches to suppress collapse in attractive BECs. Periodic modulation of the interaction strength, made possible by employing a Feshbach resonance, is predicted to partially stabilise against collapse [16], although when the average interaction is attractive, collapse is inevitable [17]. The presence of a quantized vortex is also predicted to raise the threshold for collapse [18, 19], although the presence of a vortex in an attractive condensate under harmonic trapping is not energetically stable [18, 20].

Due to the superfluid nature of BECs, it is intriguing to study their response to rotation. The rotation of repulsive BECs has been considered extensively both experimentally and theoretically (see [21] for a review). One method is to mechanically rotate the BEC in an elliptical trap [22, 23, 24] formed by time-dependent laser or magnetic fields. At low rotation frequency  $\Omega$ , the condensate remains irrotational and vortex-free. According to a hydrodynamical model, the BEC can access a family of rotating stationary solutions, characterised by a quadrupolar irrotational flow pattern [25, 26, 27, 28, 29, 30] and confirmed experimentally [23]. At a critical rotation fre-

quency, which coincides with when these irrotational solutions become unstable [28, 30], vortices are nucleated and form a vortex lattice. In the context of attractive BECs, theoretical work has shown that a centre-of-mass mode is favoured under rotation rather than the occurrence of vortices [20, 31]. Under harmonic trapping, this mode becomes excited when  $\Omega$  exceeds the trap frequency.

In this work we consider the rotation of bright solitary matter waves in an elliptical trap about the longitudinal axis. We employ a variational technique based on assuming an ansatz for the BSW profile which incorporates a quadrupolar irrotational flow pattern. By deriving the variational energy of the system, we obtain the BSW solutions and analyse their response to rotation. In particular, we find that rotation of the BSW can significantly increase the critical point for collapse.

We consider a BEC confined by an atomic “waveguide” potential, under rotation at frequency  $\Omega$  about the longitudinal axis. In the limit of zero temperature, the BEC can be described by a mean-field “wavefunction”  $\Psi(\mathbf{r}, t)$  which satisfies the Gross-Pitaevskii equation (GPE) [21],

$$i\hbar \frac{\partial \Psi}{\partial t} = \left[ -\frac{\hbar^2}{2m} \nabla^2 + V(\mathbf{r}) + g|\Psi|^2 - \Omega \hat{L}_z \right] \Psi, \quad (1)$$

where  $m$  is the atomic mass and  $g = 4\pi\hbar^2 a_s/m$  parameterizes the atomic interactions, with  $a_s$  being the s-wave scattering length. The  $\Omega \hat{L}_z$  term accounts for frame rotation, where  $\hat{L}_z = -i\hbar(x \frac{\partial}{\partial y} - y \frac{\partial}{\partial x})$  is the  $z$ -component angular momentum operator. We assume that the confining potential  $V(\mathbf{r})$  is harmonic with the form,

$$V(\mathbf{r}) = \frac{1}{2} m \omega_r^2 [(1 - \epsilon)x^2 + (1 + \epsilon)y^2 + \lambda^2 z^2], \quad (2)$$

where  $\omega_r$  is the average trap frequency in the  $x$ - $y$  plane,  $\epsilon$  is the trap ellipticity in the  $x$ - $y$  plane, and  $\lambda = \omega_z/\omega_r$  is the trap ratio that determines the axial trap strength.

In order to study the BSW solutions we employ a variational technique. This involves assuming a BSW ansatz and minimising its energy to obtain the variational solutions. This technique has been employed for non-rotating BSWs and trapped attractive BECs, and has been shown to have give very good agreement with the full solution

of the GPE. When the axial trapping is weak ( $\lambda \ll 1$ ), we will employ the *sech ansatz* for the BSW, given by,

$$\Psi_S = \sqrt{\frac{N}{2l_x l_y l_z \pi}} e^{-\frac{x^2}{2l_x^2}} e^{-\frac{y^2}{2l_y^2}} \operatorname{sech}\left(\frac{z}{l_z}\right) e^{i\alpha xy}, \quad (3)$$

where  $N$  is the atom number. Ignoring the  $e^{i\alpha xy}$  term, this ansatz is identical to that used in Refs. [6, 7, 8], with the *sech* axial profile appropriate because it is the form of the 1D soliton solution [9]. The term  $e^{i\alpha xy}$  introduces a quadrupolar flow pattern to the BEC, with  $\alpha$  determining the amplitude. This flow pattern preserves irrotationality and has been very successful in modelling vortex-free repulsive condensates under rotation [23, 26, 27, 28, 29, 30].

The total energy of the system is defined by,

$$E = \int \left[ \frac{\hbar^2}{2m} |\nabla\Psi|^2 + V(\mathbf{r})|\Psi|^2 + \frac{g}{2}|\Psi|^4 + i\hbar\Omega \left( \Psi^* x \frac{\partial\Psi}{\partial y} - \Psi y \frac{\partial\Psi^*}{\partial x} \right) \right] d^3\mathbf{r}. \quad (4)$$

Insertion of the ansatz into Eq. (4) gives the energy  $E_S$ ,

$$\begin{aligned} \frac{E_S}{N} &= \frac{\hbar^2}{2m} \left[ \frac{1}{2l_x^2} + \frac{1}{2l_y^2} + \frac{1}{3l_z^2} + \frac{l_x^2 \alpha^2}{2} + \frac{l_y^2 \alpha^2}{2} \right] \\ &+ \frac{m\omega_r^2}{4} \left[ (1-\epsilon)l_x^2 + (1+\epsilon)l_y^2 + \frac{\lambda^2 \pi^2}{6} l_z^2 \right] \\ &+ \frac{gN}{4\pi l_x l_y l_z} - \frac{\hbar\Omega_z \alpha}{2} (l_x^2 + l_y^2). \end{aligned} \quad (5)$$

We can reduce the number of variables in Eq. (5) as follows. Under the hydrodynamical interpretation, the mean-field wavefunction can be expressed as  $\Psi(\mathbf{r}, t) = \sqrt{n(\mathbf{r}, t)} \exp[i\phi(\mathbf{r}, t)]$  where  $n(\mathbf{r}, t)$  and  $\phi(\mathbf{r}, t)$  are the condensate density and phase, respectively. Furthermore,  $\mathbf{v}(\mathbf{r}, t) = (\hbar/m)\nabla\phi(\mathbf{r}, t)$  is the ‘‘fluid’’ velocity. Inserting this into the GPE and equating imaginary parts, one derives a continuity equation given by,

$$\frac{\partial n}{\partial t} + \nabla \cdot (n[\mathbf{v} - \boldsymbol{\Omega} \times \mathbf{r}]) = 0. \quad (6)$$

Our irrotational phase distribution  $\phi(\mathbf{r}) = \alpha xy$  corresponds to a velocity distribution  $\mathbf{v}(\mathbf{r}) = \hbar\alpha(y\hat{\mathbf{i}} + x\hat{\mathbf{j}})/m$ . Inserting this into the continuity equation and setting  $\partial n/\partial t = 0$ , we find that stationary solutions satisfy,

$$\alpha = \pm \frac{m\Omega_z}{\hbar} \left( \frac{l_x^2 - l_y^2}{l_x^2 + l_y^2} \right). \quad (7)$$

Note that  $\alpha$  can be positive or negative, resulting in two ‘‘branches’’ of solutions. For  $\alpha > 0$  the BSW is wider in the  $x$ -direction than in the  $y$ -direction, and vice versa for  $\alpha < 0$ . We can thus eliminate  $\alpha$  from Eq. (5). For simplicity we employ rescaled variables (in terms of the transverse harmonic oscillator)  $\gamma_x = l_x/a_r$ ,  $\gamma_y = l_y/a_r$ ,  $\gamma_z = l_z/a_r$ ,  $\tilde{\Omega} = \Omega/\omega_r$  and  $\varepsilon_S = E_S/(N\hbar\omega_r)$ , where

$a_r = \sqrt{\hbar/m\omega_r}$  is the radial harmonic oscillator length. Furthermore, we introduce the dimensionless interaction parameter  $k = N|a_s|/a_r$ . The ansatz energy becomes,

$$\begin{aligned} \varepsilon_S &= \frac{1}{4} \left[ \frac{1}{\gamma_x^2} + \frac{1}{\gamma_y^2} + \frac{2}{3\gamma_z^2} \right. \\ &+ (1-\epsilon)\gamma_x^2 + (1+\epsilon)\gamma_y^2 + \frac{\lambda^2 \pi^2}{6} \gamma_z^2 \left. \right] \\ &- \frac{k}{3\gamma_x \gamma_y \gamma_z} \pm \frac{\tilde{\Omega}_z^2}{4} [\gamma_x^2 - \gamma_y^2] \left[ \frac{\gamma_x^2 - \gamma_y^2}{\gamma_x^2 + \gamma_y^2} - 2 \right]. \end{aligned} \quad (8)$$

Recall that Eq. (8) is valid for  $\lambda \ll 1$ . Under tight axial trapping  $\lambda \gg 0$ , this direction is dominated by the trap rather than the interactions and it is more appropriate to consider a *gaussian ansatz*,

$$\Psi_G = \sqrt{\frac{N}{l_x l_y l_z \pi^{3/2}}} e^{-\frac{x^2}{2l_x^2}} e^{-\frac{y^2}{2l_y^2}} e^{-\frac{z^2}{2l_z^2}} e^{i\alpha xy}. \quad (9)$$

The rescaled energy for the gaussian ansatz is then,

$$\begin{aligned} \varepsilon_G &= \frac{1}{4} \left[ \frac{1}{\gamma_x^2} + \frac{1}{\gamma_y^2} + \frac{1}{\gamma_z^2} \right. \\ &+ (1-\epsilon)\gamma_x^2 + (1+\epsilon)\gamma_y^2 + \lambda^2 \gamma_z^2 \left. \right] \\ &- \frac{k}{\sqrt{2\pi} \gamma_x \gamma_y \gamma_z} \pm \frac{\tilde{\Omega}_z^2}{4} [\gamma_x^2 - \gamma_y^2] \left[ \frac{\gamma_x^2 - \gamma_y^2}{\gamma_x^2 + \gamma_y^2} - 2 \right] \end{aligned} \quad (10)$$

Note that, for the regimes of interest, the *sech* and gaussian ansatz give similar results, typically differing by less than 10% [8]. We can now map out the 3D energy landscapes of the rotating BSWs as a function of the lengthscales  $\gamma_x$ ,  $\gamma_y$  and  $\gamma_z$ . Variational BSW solutions exist where there is a local energy minimum in the landscape, and are obtained by a numerical search algorithm. The local energy minimum has widths  $\gamma_x^0$ ,  $\gamma_y^0$  and  $\gamma_z^0$ , energy  $\varepsilon_0$ , and quadrupolar flow amplitude  $\alpha_0$ .

We first revisit the  $\lambda = 0$  BSW solutions in the absence of rotation and ellipticity, as studied previously using the

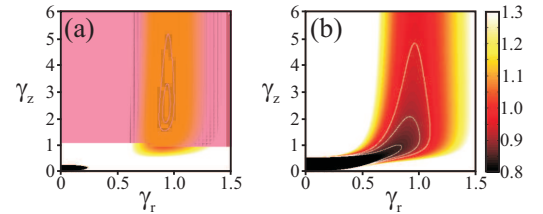


FIG. 1: Energy landscape of the non-rotating and non-elliptical system for  $\lambda = 0$  according to Eq. (8). (a) Stable regime  $k = 0.4 < k_c$  featuring a local energy minimum, i.e. the BSW solution. (b) Unstable regime  $k = 0.8 > k_c$ , where the whole parameter space is unstable to collapse. White contours highlight the shape of the landscapes. Since Eq. (8) is cylindrically symmetric in this case, we introduce a radial lengthscale  $\gamma_r = \sqrt{(\gamma_x^2 + \gamma_y^2)}/2$ .

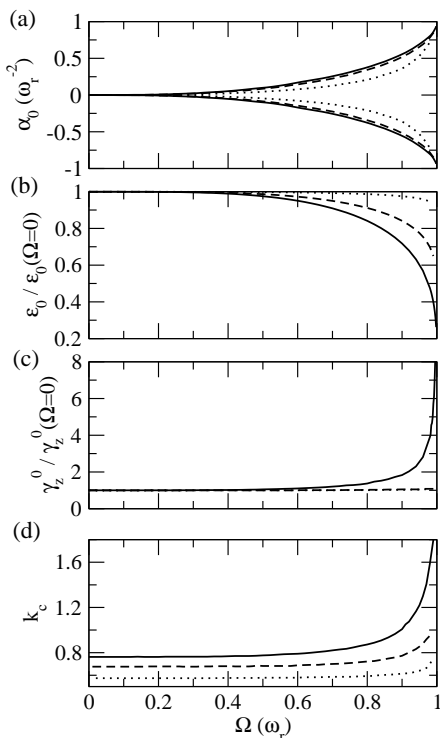


FIG. 2: Properties of  $\epsilon = 0$  BSW solutions as a function of  $\Omega$  for  $\lambda = 0$  (solid line) and the axially-trapped cases of  $\lambda = 1$  (dashed lines) and  $\lambda = 5$  (dotted lines). (a) Quadrupolar flow amplitude  $\alpha_0$  for interaction parameter  $k = 0.4$ . (b) BSW energy  $\epsilon_0$  for  $k = 0.4$ . (c) Axial lengthscale  $\gamma_z^0$  for  $k = 0.4$ . (d) Critical interaction parameter for collapse  $k_c$ . Note that for  $\lambda = 0$  ( $\lambda > 0$ ) we employ the sech (gaussian) ansatz.

$\alpha = 0$  limits of Eq. (8) [6, 8] and Eq. (10) [4]. Here the energy landscape is cylindrically symmetric ( $\epsilon = 0$ ) and so we introduce a radial lengthscale  $\gamma_r = \sqrt{(\gamma_x^2 + \gamma_y^2)}/2$ . A typical energy landscape, according to Eq. (8), for a stable BSW solution is presented in Fig. 1(a), corresponding to  $k = 0.4$ . At the origin the interaction term in Eq. (8) diverges to negative values and is a region of collapse of the BSW. However, there exists a local energy minimum which represents the self-trapped BSW solution. A typical unstable energy landscape is shown in Fig. 1(b) for  $k = 0.8$ . No local energy minimum exists, and the whole parameter space is unstable to collapse. From this the critical interaction strength for collapse is determined to be  $k_c = 0.76$ , in good agreement with full solution of the GPE which gives  $k_c \approx 0.68$  [6, 8].

We will now consider the effect of rotation. For simplicity we first assume  $\epsilon = 0$ . Figure 2(a)-(c) shows how the key parameters vary as rotation is introduced for a fixed interaction parameter  $k = 0.4$ . For  $\Omega > 0$  the symmetry between  $\gamma_x$  and  $\gamma_y$  is broken and the solutions have non-zero  $\alpha_0$  (Fig. 2(a)). We see the formation of two branches of  $\alpha_0$ . Due to the trap symmetry in the  $x$ - $y$  plane, the branches are symmetric about the  $\alpha_0 = 0$  axis, with the upper branch being elongated in the  $x$ -

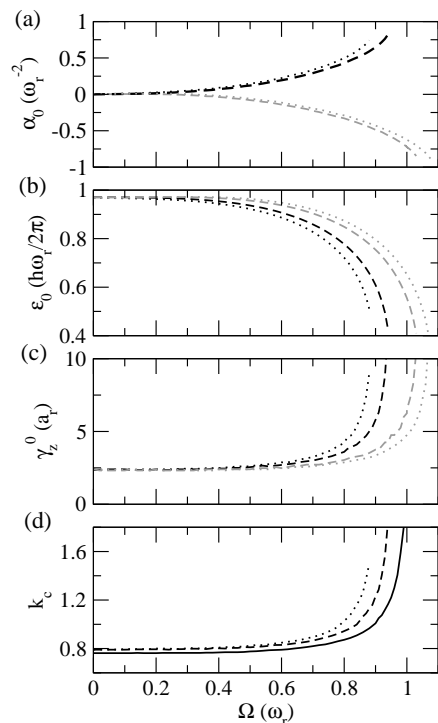


FIG. 3: Properties of the rotating  $\lambda = 0$  BSWs for elliptical traps of  $\epsilon = 0.1$  (dashed lines) and  $0.2$  (dotted lines). Black (grey) lines indicate upper (lower) branch solutions. (a) Quadrupolar flow amplitude  $\alpha_0$  for  $k = 0.4$ . (b) BSW energies  $\epsilon_0$ , rescaled by their non-rotating values of  $\epsilon_0(\Omega = 0) = 0.972$  for  $\lambda = 0$ ,  $1.315$  for  $\lambda = 1$  and  $3.01$  for  $\lambda = 5$ . (c) Axial lengthscales  $\gamma_z^0$ , rescaled by  $\gamma_z^0(\Omega = 0) = 2.36$  for  $\lambda = 0$ ,  $0.902$  for  $\lambda = 1$  and  $0.416$  for  $\lambda = 5$ . (d) Critical interaction parameter for collapse  $k_c$  of the upper branch (lowest energy) solutions.

direction and the lower branch being elongated in the  $y$ -direction. As  $\Omega$  increases, so too does the magnitude of  $\alpha_0$ , implying a spreading of the BSW in the  $x$ - $y$  plane. This is because of the growth of an outward centrifugal force. As  $\Omega$  approaches  $\omega_r$ ,  $\alpha_0$  diverges to  $\pm\infty$ . This is because, at  $\Omega = \omega_r$ , the centrifugal force exactly balances the trapping potential, and the BEC is untrapped in the  $x$ - $y$  plane. Since the BEC centre-of-mass becomes dynamically unstable, this is termed the *centre-of-mass instability* [32]. The BSW energy (Fig. 2(b)) decreases towards zero as  $\Omega \rightarrow \omega_r$  as a result of the reduced density. The axial lengthscale (Fig. 2(c)) grows with  $\Omega$  since the radial spreading dilutes the interaction strength and forms a less tightly bound BSW.

We have isolated the critical interaction parameter for collapse  $k_c$  as a function of  $\Omega$  with the results shown in Fig. 2(d). The most striking feature is that  $k_c$  dramatically increases as  $\Omega_z$  approaches  $\omega_r$ . This is directly associated with the radial spreading and reduced density of the rotating solutions. Specifically, for  $\Omega/\omega_r = 0.9$ ,  $k_c$  is approximately 50% larger than its non-rotating value while for  $\Omega/\omega_r = 0.97$ ,  $k_c$  is approximately twice as large.

In Fig. 2 we also consider the presence of significant

axial trapping  $\lambda = 1$  (dashed line) and 5 (dotted line), for which we employ the gaussian ansatz. We see similar qualitative behaviour to the  $\lambda = 0$  case: a divergent growth of  $\alpha_0$  (Fig. 2(a)) and decrease in  $\epsilon_0$  (Fig. 2(b)). However, the magnitudes are consistently less than the corresponding  $\lambda = 0$  results. The axial lengthscales (Fig. 2(c)) show little variation with  $\Omega$  since this is now dominated by the external axial trapping. The critical point for collapse  $k_c$  grows with  $\Omega$ , but at a slower rate than for  $\lambda = 0$ . Note that the presence of axial trapping reduces  $k_c$ , as observed elsewhere [8, 13].

The  $\epsilon = 0$  limit is somewhat unphysical since no torque is actually applied to the BEC. We now consider the more realistic case of finite trap ellipticity. The results for  $\lambda = 0$  BSWs under  $\epsilon = 0.1$  and  $0.2$  are presented in Fig. 3. The finite ellipticity breaks the symmetry in the  $x$ - $y$  plane and therefore in the branches of  $\alpha_0$ . The upper branch solutions are elongated in the  $x$ -direction, which has trap frequency  $\omega_x = \sqrt{(1-\epsilon)\omega_r}$ . The centre-of-mass instability then occurs when  $\Omega = \sqrt{(1-\epsilon)\omega_r}$ , which is why the divergence in  $\alpha_0$  shifts to lower  $\Omega$ . Conversely, the lower branch solutions diverge at  $\Omega = \sqrt{1+\epsilon\omega_r}$  and so become shifted towards larger  $\Omega$ .

Consideration of the energy (Fig. 3(b)) shows that the upper branch solutions have lower energy. That is, it is

lower energy for the condensate to be elongated in  $x$  than  $y$ , since the trap is weaker in this direction. Consequently, we expect that only the upper branch solutions would ever be observed. Apart from the shift in the asymptotes introduced by the finite ellipticity, the behaviour of  $\alpha_0$ ,  $\epsilon_0$  and  $\lambda_z^0$  is qualitatively and quantitatively similar to the  $\epsilon = 0$  case. In Fig. 2(d) we plot the critical interaction parameter for collapse  $k_c$  of the upper branch solutions. Again, we see similar behaviour to the  $\epsilon = 0$  case, with a dramatic increase in  $k_c$  as  $\Omega$  approaches  $\sqrt{1-\epsilon\omega_r}$ .

In this work we have employed a variational technique to study bright solitary matter-wave solutions under rotation in elliptical traps. This is made possible by incorporating an irrotational quadrupolar flow pattern into the variational ansatz. Importantly, the BSW becomes more stable to the collapse instability when under rotation. This is most pronounced when the rotation frequency  $\Omega$  is slightly less than the minimum effective trap frequency  $\sqrt{1-\epsilon\omega_r}$ , e.g., for  $\Omega = 0.9\sqrt{1-\epsilon\omega_r}$ , the critical interaction parameter for collapse  $k_c$  increases by approximately 50% over the non-rotating value. This implies that the BSW can support the same increase in number of atoms, before collapse.

We acknowledge funding from the ARC and the Canadian Commonwealth Scholarship Program (NGP).

- 
- [1] K.E. Strecker *et al.*, Nature **417**, 150 (2002).  
[2] L. Khaykovich *et al.*, Science **296**, 1290 (2002).  
[3] S.L. Cornish, S.T. Thompson and C.E. Wieman, Phys. Rev. Lett. **96**, 170401 (2006).  
[4] V.M. Pérez-García, H. Michinel, J.I. Cirac, M. Lewenstein and P. Zoller, Phys. Rev. A **56**, 1424 (1997).  
[5] V.M. Pérez-García, H. Michinel and H. Herrero, Phys. Rev. A, **57**, 3837 (1998).  
[6] L.D. Carr and Y. Castin, Phys. Rev. A **66**, 063602 (2002).  
[7] L. Salasnich, A. Parola and L. Reatto, Phys. Rev. A **66**, 043603 (2002).  
[8] N. G. Parker, S. L. Cornish, C. S. Adams and A. M. Martin, J. Phys. B **40**, 3127 (2007).  
[9] V. E. Zakharov and A. B. Shabat, Sov. Phys. JETP **34**, 62 (1972).  
[10] P. Nozières and D. Pines, *Theory of Quantum Liquids Vol. II* (Addison-Wesley, Redwood City)  
[11] C.C. Bradley, C.A. Sackett and R.G. Hulet, Phys. Rev. Lett. **78**, 985 (1997).  
[12] J.L. Roberts *et al.*, Phys. Rev. Lett. **86**, 4211 (2001).  
[13] A. Gammal, T. Frederico and L. Tomio, Phys. Rev. A **64**, 055602 (2001); A. Gammal, L. Tomio and T. Frederico, Phys. Rev. A **66**, 043619 (2002).  
[14] N. G. Parker, A. M. Martin, S. L. Cornish and C. S. Adams, J. Phys. B **41**, 045303 (2008).  
[15] L. D. Carr and J. Brand, Phys. Rev. Lett. **92**, 040401 (2004); Phys. Rev. A **70**, 053613 (2004).  
[16] H. Saito and M. Ueda, Phys. Rev. Lett. **90**, 040403 (2003); F. K. Abdullaev *et al.*, Phys. Rev. A **67**, 013605 (2003); S. K. Adhikari, Phys. Rev. A **69**, 063613 (2004); G. D. Montesinos, V. M. Perez-Garcia and P. J. Torres, Physica **191D**, 193 (2004).  
[17] V. V. Konotop and P. Pacciani, Phys. Rev. Lett. **94**, 240405 (2005).  
[18] F. Dalfovo and S. Stringari, Phys. Rev. A **53**, 2477 (1996).  
[19] S. K. Adhikari, New J. Phys. **5**, 137 (2003).  
[20] N. K. Wilkin, J. M. F. Gunn and R. A. Smith, Phys. Rev. Lett. **80**, 2265 (1998).  
[21] P. G. Kevrekidis, D. J. Frantzeskakis and R. Carretero-Gonzalez (Eds.), *Emergent Nonlinear Phenomena in Bose-Einstein Condensates: Theory and Experiment* (Springer, 2008).  
[22] K. W. Madison, F. Chevy, W. Wohlleben and J. Dalibard, Phys. Rev. Lett. **84**, 806 (2000).  
[23] K. W. Madison, F. Chevy, V. Bretin and J. Dalibard, Phys. Rev. Lett. **86**, 4443 (2001).  
[24] E. Hodby *et al.*, Phys. Rev. Lett. **88**, 010405 (2001).  
[25] Y. Castin and R. Dum, Eur. Phys. J. D **7**, 399 (1999).  
[26] A. Recati, F. Zambelli and S. Stringari, Phys. Rev. Lett. **86**, 377 (2001).  
[27] S. Sinha and Y. Castin, Phys. Rev. Lett. **87**, 190402 (2001).  
[28] N. G. Parker, R. M. W. van Bijnen and A.M. Martin, Phys. Rev. A **73**, 061603(R) (2006).  
[29] R.M.W. van Bijnen, D.H.J. O'Dell, N.G. Parker and A.M. Martin, Phys. Rev. Lett. **98**, 150401 (2007).  
[30] I. Corro, N. G. Parker and A. M. Martin, J. Phys. B **40**, 3615 (2007).  
[31] A. Collin, E. Lundh and K.-A. Suominen, Phys. Rev. A **71**, 023613 (2005); A. Collin, Phys. Rev. A **73**, 013611 (2006).  
[32] P. Rosenbusch *et al.*, Phys. Rev. Lett. **88**, 250403 (2002); N. G. Parker and C. S. Adams, J. Phys. B **39**, 43 (2006).